LONG-TERM ATMOSPHERIC CORROSION
STUDIES BASED TO THE ETHNOGRAPHIC OBJECTS
DATED XVIII – XIX CENTURIES

ABSTRACT

THESIS

Long-term atmospheric corrosion has become in recent decades, a very important theme in several fields. Properties of oxides formed on the surface of ferrous objects interest in:

- the conservation - restoration, in an attempt to prolong the life of objects produced centuries ago, evidence of identity and culture of a people;
- materials science, for understanding the mechanisms that occur at the interface of metal – medium and in understanding physicochemical and mechanical properties, predicting the future behavior of actual appliances and mechanisms;
- biology, for understanding the mechanisms of interaction between fine particles and organic systems plus their environmental impact;
- chemistry, in understanding the oxidation-reduction and acid-base surface, controlled environment and nature of cations is often crucial for applications in heterogeneous catalysis.

The most relevant resources to analyze this domain, in addition to laboratory environments – artificially created, are the artifacts made only of iron – household items, with functional and decorative role – or iron combined with other materials, like tools with wooden handle, but also like the consolidation or reinforcing element, in wooden buildings.

The paper is structured in two directions: a theoretical and an experimental set over the seven chapters:

In the beginning of understanding the evolution of long-term atmospheric corrosion, a short presentation of the iron processing technology was required, during the period considered, XVIII - XIX centuries, starting right from the two traditional methods of ore reduction - in lower furnace (Fig. 1.) and blast furnace (Fig. 2).

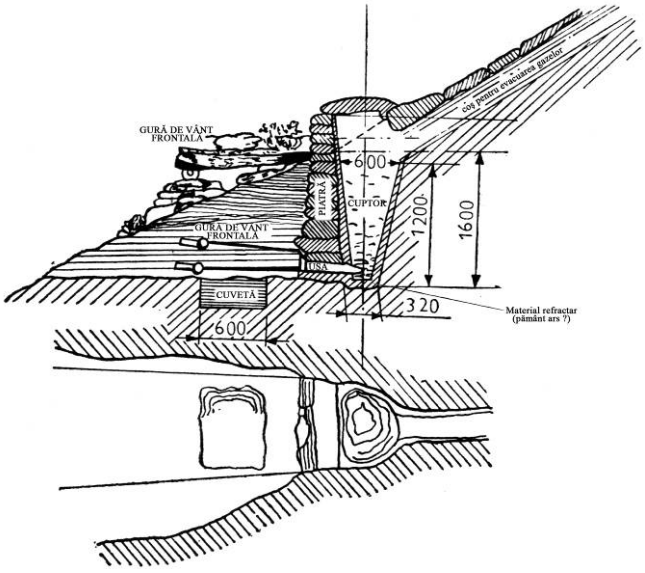

Fig. 1. Furnace for reducing iron ore (IX centuries), discovered in Valea Caselor, Ghelar, apud rev. *Natura*, 1930, nr. 6, p. 30

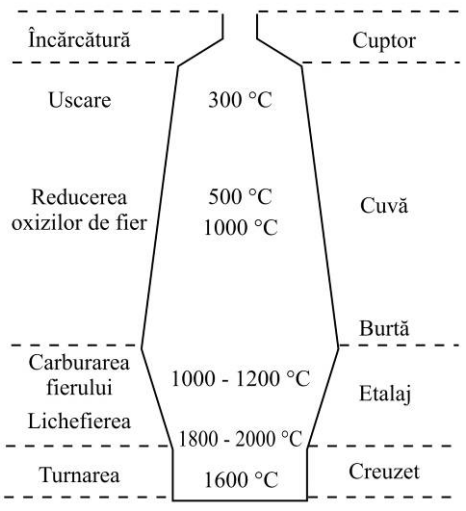

Fig. 2. Schematic diagram of the blast furnace

It is followed by the presentation of some traditional methods of processing iron, as: hammering, cutting, stamping, perforation, riveting, incision, welding, but also of the empirical heat treatments: hardening and carburizing.

It was presented a classification of the objects made iron or steel, taking into consideration, firstly, their production "technique", followed, in the end of chapter I, by the presentation of three techniques of achieving: a dig, a scythe and a harvest – all descriptions were made by the artisan blacksmiths.

In further research, in Chapter II, it was appealed to the relationship presentation, which was created over time, between corrozists and conservatives – restorers, and as well the presentation of two models of approaching the corrosion. We refer to the one proposed by Graedel, under the acronym GILDES (Gas, Interface, Liquid Deposition, Layer, Electrode regimes, solid) and one more complex, proposed by I. S. Cole, where the scale defined by EOTA[1] (1997) was respected, so that macro refers to gross meteorological conditions (polar, subtropical etc.), meso refers to regions with dimensions up to 100 km, local is in the immediate vicinity of a building, while micro refers to the absolute proximity of a material surface.

Once again, stressing the importance of understanding the mechanism of corrosion to the iron objects, the end of Chapter II was dedicated to defining the notion LIMITOS (Limit of the Original Surface), which is the limit between the different materials which have constituted the object (metallic, minerals and organics) and the soils where were abandoned. So, the corrosion layer can be located under the LIMITOS and is recognized because it contains "internal markers" which proceed of the metallic support (eg. slag inclusions) or above the LIMITOS, recognized by "external markers" like minerals in soils (eg. quartz grains) (Fig. 3).

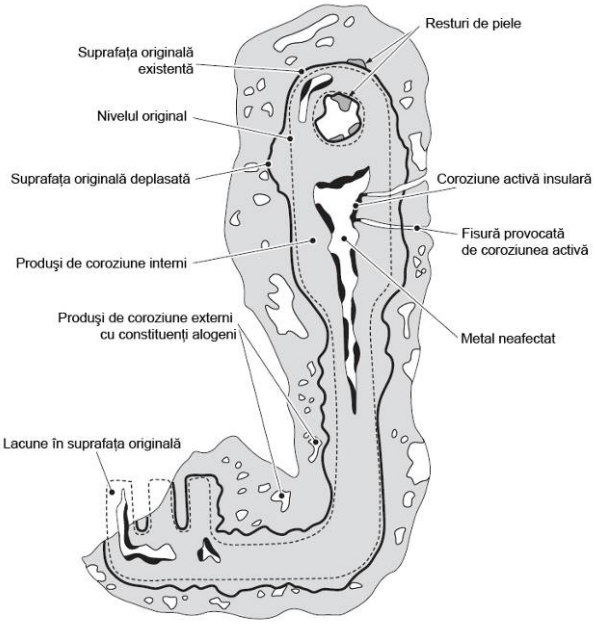

Fig. 3. Section of a key archaeological [2]

Chapter III was destined for introduction in the context to the studies. Here, was defined the notion of atmospheric corrosion, where was underlined environmental influence, starting from climatic conditions.

[1] EOTA (European Organisation for Technical Approvals)
[2] Philippe Dillmann, *Corrosion des objets archéologique ferreux*, COR – 675, p. 3.

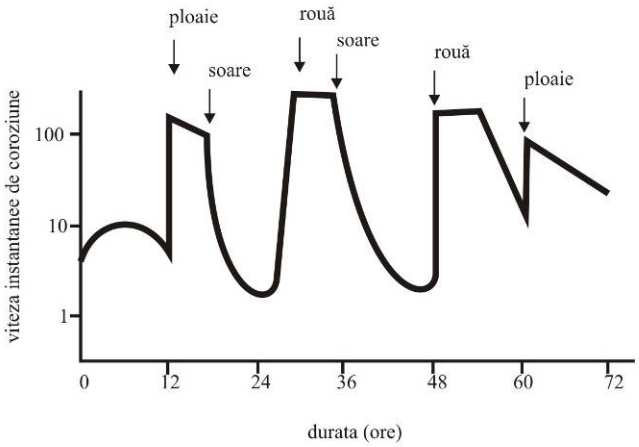

Fig. 4. Variation instantaneous velocity of corrosion of iron depending on climatic conditions [3]

It was continued with a very important factor regarding humidity, namely ***wet period***[4], followed by ***convection effect*** (air movement at object surface), as well as ***conduction effect*** (inside object), so could have highlighted the influence of wind speed, as an obvious limiting factor

Were analyzed influences changes in heat, also saturated vapor pressure and air pollutants.

Also, was presented nanoscopic reaction diagram the formation of rust.

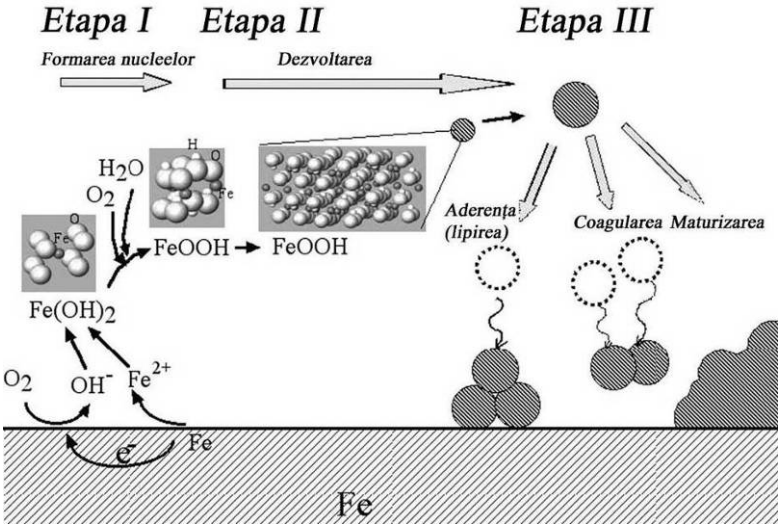

Fig. 5. Nanoscopic reaction diagram the formation of rust [5].

In this chapter a thermodynamic approach was also presented – given by Pourbaix diagrams, being exposed those that have been developed for systems containing compounds often found in industrial-urban atmosphere: carbon dioxide, phosphates and chlorides

It was necessary to present several types of corrosion, respectively the most common found on ethnographic objects, which form the subject research, with examples on these types of objects: cavernous, peeling, filiform, differentiated, in paint, the effect of crevice, under pressure, and the last, fragility due to hydrogen.

---

[3] Judith Monnier, *Corrosion atmosphérique sous abri d'alliages ferreux historique*, these de Docteur, Paris, 2008, p. 12, apud Dieter Landolt, *Traite des matériaux, corrosion et chimie de surfaces des métaux*, 2003, Lausanne

[4] Philip A. Schweitzer, *Fundamentals of metallic corrosion. Atmospheric and media corrosion of metals*, CRC Press Taylor and Francis Group, p. 42.

[5] H. Kihira, *Colloidal Aspects of Rusting of Weathering Steel. H. Ohshima*, K. Furusawa, *Electrical Phenomena at Interfaces, Fundamentals, Measurements and Applications.* -2nd ed. Macel Dekker, Inc., New York, 1998, p.429 – 440

Once the atmospheric corrosion was submitted, it was passed, in Chapter IV, to the presentation of iron compounds which are likely to form the layer of corrosion products: the three oxides – *magnetite* **Fe_3O_4** (level of oxidation II and III), *hematite* **α-Fe_2O_3** (level of oxidation III) and *maghemite* **γ-Fe_2O_3** (degree of oxidation III)[6], the ferrous and ferric hydroxides and also iron oxi-hydroxides, in number 4: *goethite* **α-FeO(OH)**, *akaganeite* **β-FeO(OH)**, *lepidocrocite* **γ-FeO(OH)** and *feroxihite* **δ-FeO(OH)**, all with the degree of oxidation III.

Next, the main proprieties of the corrosion products were presented: solubility (fig. 6.) and conductivity.

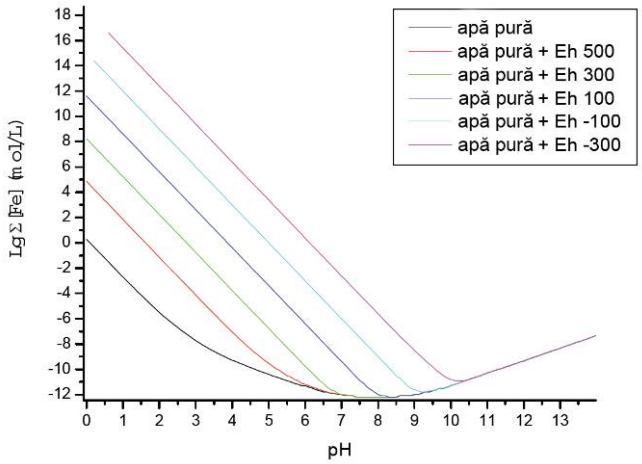

Fig. 6. Goethite solubility in pure water depending on pH

The end of this chapter, the last from the theoretical direction, was destined to a brief description of short-term atmospheric corrosion (< 20 years) and also a brief description of a model of indoor atmospheric corrosion[7].

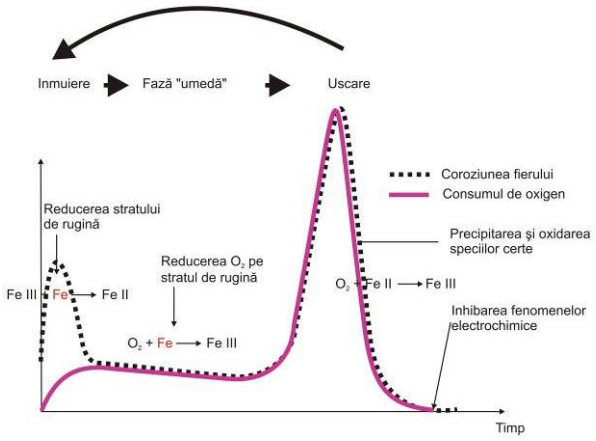

Fig. 7. Wetting and drying cycle[8]

The second research direction, contained in Chapters V – VII (Study system, models analysis and experimental methods, Presentation of results, Interpretation of results) was focused on experimental study, a number of 17 pieces being analyzed, after the scheme:

---

[6] Wustita, FeO, este, de asemenea, un oxid de fier. Cu toate acestea, datorită faptului că se formează la temperaturi superioare celei de 570 ˚C, nu va fi luată în considerare la analiza coroziunii atmosferice.

[7] S. Hoerlé, F. Mazaudier, Ph. Dillmann, G. Santarini, *Advances in understanding atmospheric corrosion of iron. II. Mechanistic modeling of wet–dry cycles*, Corrosion Science 46 (2004), p. 1431 – 1465.

[8] M. Stratmann, H. Streckel, *On the atmospheric corrosion of metals which are covered with thin electrolyte layers—I. Verification of the experimental technique,* Corrosion Science, Volume 30, Issues 6 - 7, 1990, p. 688

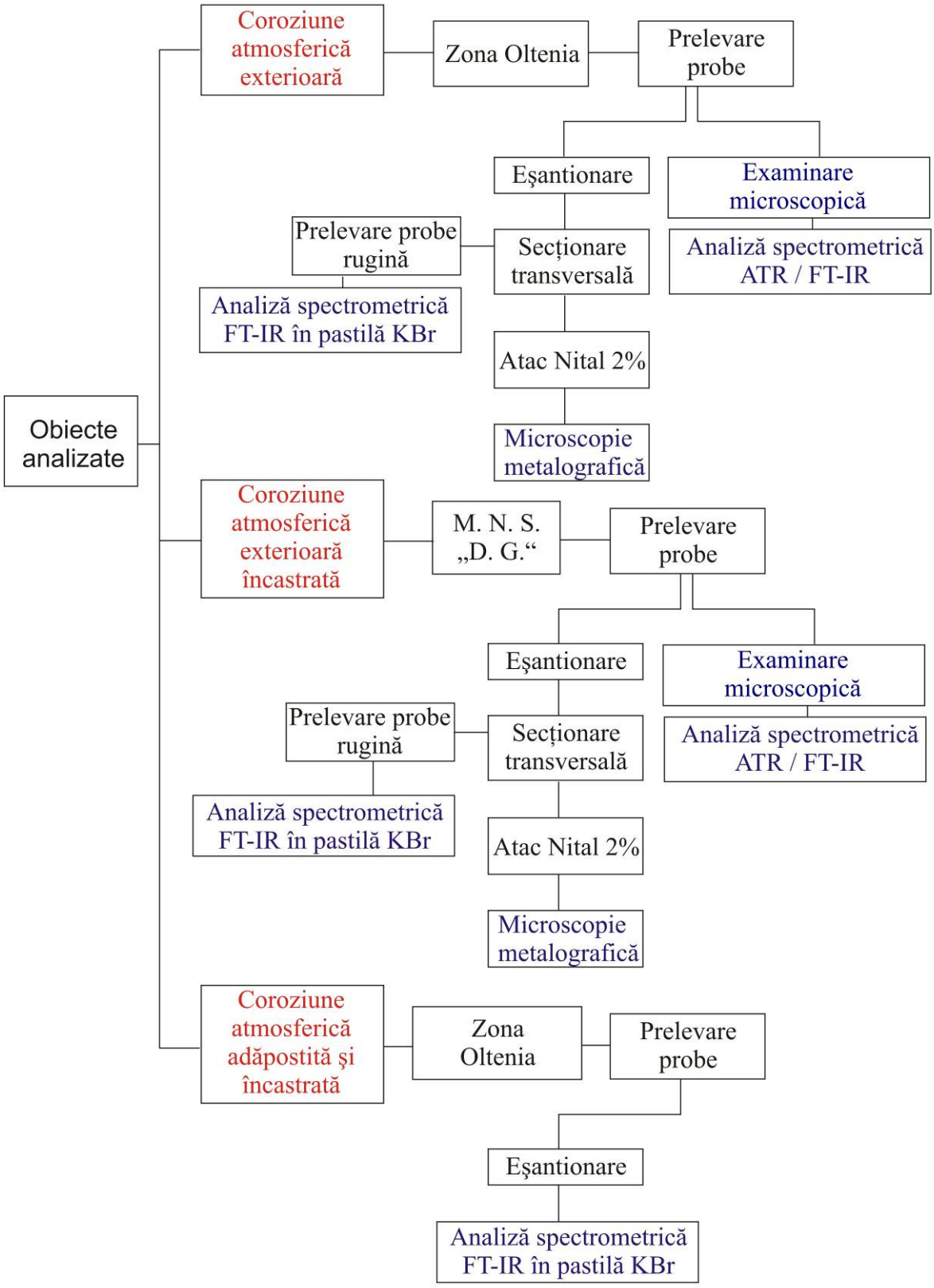

Fig. 8. Proposed experimental program

Analyzing instruments used were the metallographic, stereomicroscopic and those made by FT-IR.

Analyzing method, Fourier Transform Infrared Spectroscopy (FT-IR), was chosen because it is a powerful tool for identifying chemical bonds in the molecule by submitting an *Infrared absorption spectrum*, which is like a molecular "footprint", and also because it allows identifying the main corrosion products: goethite and lepidocrocite.

IR spectra are useful, particularly in the final identification of certain species such as FeOOH, which are strongly paramagnetic at room temperature and, therefore, γ-FeOOH indistinguishable by Mössbauer spectrometry.

In addition, at the temperature of liquid nitrogen, α-FeOOH has a similar field to Magnetite's and therefore, its Mössbauer spectrum overlaps the Magnetite's. Similarly, ultra-fine particles of α-FeOOH are amorphous under X-rays and therefore can not appear in XRD patterns[9].

Analyzed objects were grouped by the type of corrosion that they have been supposed to:

In the first group, destined to the ***external atmospheric corrosion***, a number of seven pieces were analyzed, to which were added to two samples of corrosion products taken from the outer grid of a window and a church's cross.

Fig. 9. Hook, 3/4 19th century, D = 82 mm; $d_{secțiune}$ = 15 mm

Fig. 10. Short chisel, ¼ 19th century, L = 124 mm; $l_{lamă}$ = 30 mm; D = 35 mm

Fig. 11. Chain hearth, 4/4 19 th century, L = 140 mm; $l_{latură\ secțiune\ pătrată}$ = 7 mm

Fig. 12. Spike of carpentry - sectioned, 2/4 20th century, L = 170 mm; l = 16 mm

Fig. 13. Pawl; 4/4 19th century; L = 300 mm; $l_{latură\ secțiune\ pătrată}$ = 9 mm

Fig. 14. Hardware tool (for cutting and punching); 4/4 19th century; L = 180 mm; l = 27 mm

[9] R. Balasubramaniam, A. V. Ramesh Kumar, P. Dillmann, *Characterization of rust on ancient Indian iron*, în Current Science, Vol. 85, No. 11, 2003, p. 1550 passim.

Fig. 15. Corrosion products taken from the window's grid, nave, wooden church Dragomireşti, Maramures County, dated 1722, located from 1936 in the National Village Museum "Dimitrie Gusti"

Fig. 16. Corrosion products taken from the cross on the porch, the east area, the wooden church Dragomireşti, Maramures County, dated 1722, located from 1936 in the National Village Museum "Dimitrie Gusti"

The second group, destined to ***the corrosion of iron embedding in wood product,*** under an ***external atmosphere***, was composed of 5 objects, all nail-like, as follows:

Fig. 17. Nail, gate wooden church Răpciuni, Neamț county, dated 1773, in 1936, displaced in the National Village Museum "Dimitrie Gusti"

Fig. 18. Nail, beams porch, N side, western wood Church Dragomireşti, Maramures County, dated 1722, displaced in the 1936 MNS "DG" total length 55 mm, dimensions 5 x 4 mm base

Fig. 19. Nail, beams porch, N side, wooden church southernmost Dragomireşti, Maramures County, dated 1722, displaced in the 1936 MNS "DG" total length 55 mm, base dimensions 3 x 2 mm

Fig. 20. Nail, access pillar of the porch, side V Dragomireşti northern tip of the wooden church, Maramures County, dated 1722, displaced in the 1936 MNS "DG" total length of 18 mm, 0.92 mm diameter

Fig. 21. Nail, porch, N side, western wood Church Timişeni, Gorj County, dated 1773, displaced in the 2002 MNS "DG" total length 30 mm, 1.4 mm diameter

The third group focused on the analysis of corrosion compounds formed on the iron embedded in wood, in indoor atmosphere. We refer to 4 hanging systems of household objects, all embedded in lime wood.

Fig. 21. Hangers – hook type, 19th century, originating from the Dolj County. Nail, made from a strip, L = 42 mm, l_{max} = 4 mm.

Fig. 22. Hangers – "clip" type, 19th century, originating from the Dolj County. It made from a strip, L = 40 mm.

Fig. 23. Hangers – hook type, 18th century, originating from the Dolj County. It made from a strip, L = 56 mm, with square section

Fig. 24. Nail, 18th century, originating from the Dolj County, L = 22 mm, with square section

The results, presented in Chapter VI, have been grouped by the three types of analyzed corrosion and by the type of analysis performed:

Micrographic, preserving the classic line, was carried on the surface of metal support. The results were presented for each sample. For example, the result for the first part of group II:

Sample B : 1

To nail B:1, two areas were analyzed: the first area – head nail, the second area: embedding area.

In the first area, the nail presents nonmetalic inclusions – fine silicates, STAS 5949-80, cu punctaj mai mare de 5 scara "a"

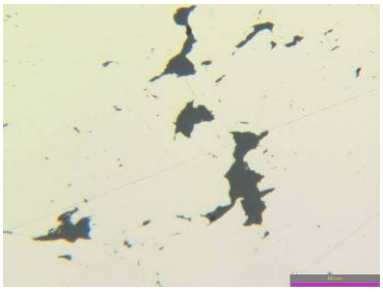

Fig. 25. 100:1

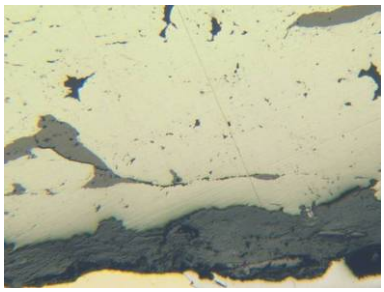

Fig. 26. 50:1

Throughout the first area of nail, can be observed iron oxides – FeO (wüstite), inside the metal mass.

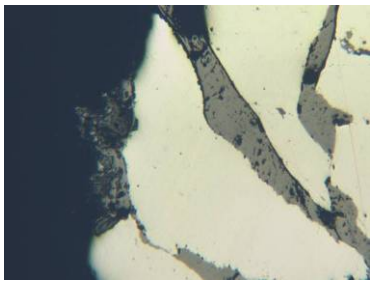

Fig. 27. 50:1

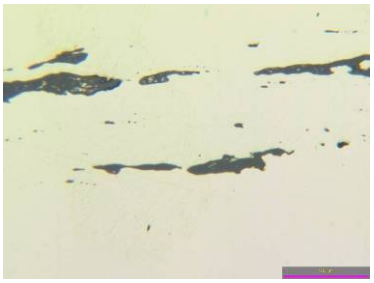

Fig. 28. 100:1

In the embedding area, the nail present nonmetallic inclusions - fine silicates, consider, with a score greater than 5.

After etchant Nital 2%, the head nail shows a microstructure consisting of grain of ferrite and perlite (Fig. 29). Grain is determined by six points according to ISO 643-93. In the embedding area, microstructure is an overheating aspect – Widmanstätten type. Outwards (Fig. 30) observed a higher proportion of perlite, probably due to carburizing heating products for forging, which was made in wood charcoal. Inwards, (Fig. 31), microstructure consists of needle ferrite and perlite (Widmanstätten structure type)

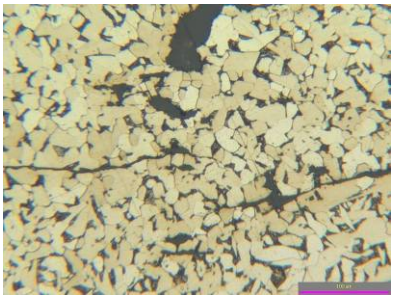

Fig. 29. 100:1 Etchant: Nital 2%

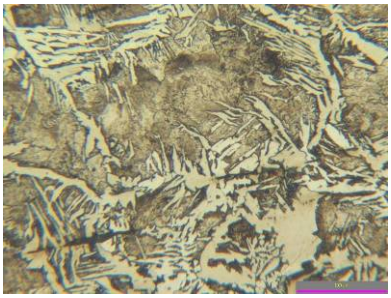

Fig. 30. 100:1 Etchant: Nital 2%

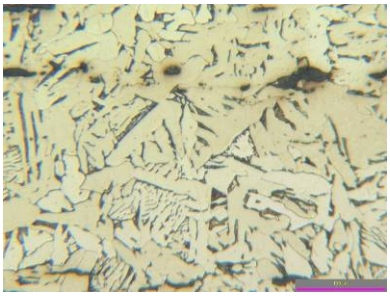

Fig. 31. 100:1 Etchant: Nital 2%

The stereomicroscopie was performed on the corrosion products, in reflected light, plane-epipolarized light and in epi-fluorescent UV light: for example – de sample A:8

Fig. 32. Product sample area (reflected light, 60x)

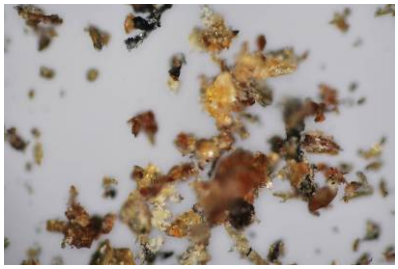

Fig. 33. plane-epipolarized light (100x)

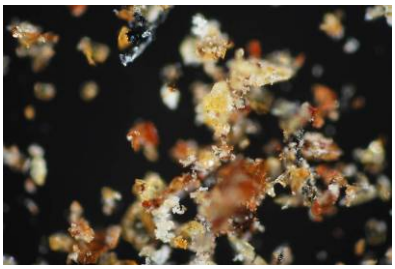

Fig. 34. Crossfire epipolarized light (100x)

And FT-IR spectroscopy was performed, for all objects, mentioning that for the second group of objects, analysis was done for both free and for the embedded area.

Each spectrum has been interpreted.

For example, sample A:7:

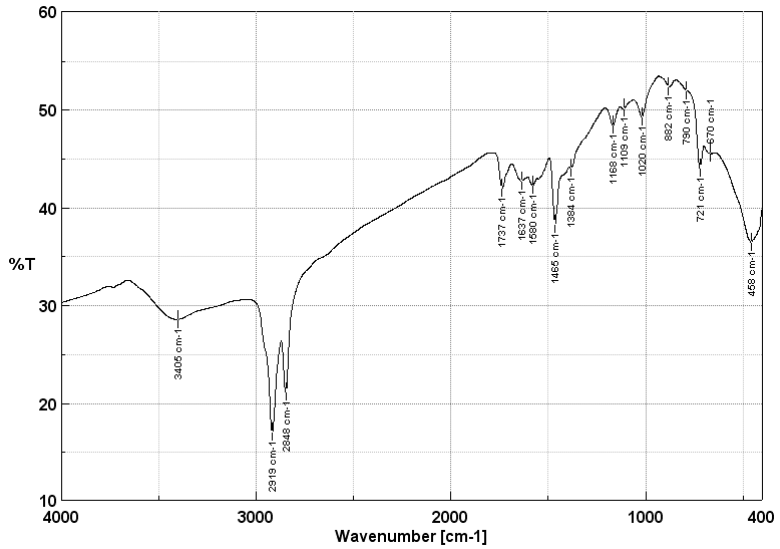

Fig. 35. The FTIR spectra, in KBr capsule, sample A:7

Goethite presence is identified using bands 790 cm^{-1} şi 882 cm^{-1}. Lepidocrocite was identified by the band from 1020 cm^{-1}, also akaganeite to 721 cm^{-1}. It can also be observed the feroxihit by the presence of peak at 458 cm^{-1}. Aliphatic hydrocarbons are also present in the band at 1384 cm^{-1}. The peaks from 2848 cm^{-1} and 2919 cm^{-1} highlights the hydrocarbons presence (CH_2 or CH_3), carbonates at 1465 cm^{-1}, and 1109 cm^{-1} is attributed glicosides (cellulosic compound)[10]. The peak presence at 672 cm^{-1} is characteristic for anthophyllite. Ferric phosphate ($FePO_4 \cdot 2H_2O$) is also present in peak[11] 1168 cm^{-1}. The IR band at 3405 cm^{-1} is due to chains of H_2O molecules and OH groups, while band 1637 cm^{-1} is due to molecular vibration transmission de H_2O or OH^- group. Peak formed at 1580 cm^{-1} is assigned to COO-Fe[12].

Chapter VII was dedicated to interpreting the results.

In this chapter the results of tests carried out using SEM-EDS on inclusions in the metal substrate samples, bellow (see table).

	MgO	Al_2O_3	SiO_2	P_2O_5	SO_3	K_2O	CaO	TiO_2	V_2O_5	Cr_2O_3	MnO	FeO
A:1	0,41	0,29	12,45	2,65	0,21	0,87	1,78	0,15	0,12	0,14	0,41	80,29
A:2	0,84	0,31	14,40	5,95	0,12	0,59	2,70	0,19	0,15	0,09	0,50	80,38
A:3	0,36	0,49	19,19	7,32	0,61	0,72	2,10	0,14	0,13	0,08	0,36	68,30
A:4	0,26	0,38	18,13	6,23	0,26	0,27	1,91	0,14	0,11	0,10	0,37	71,63
A:6	0,13	0,30	18,08	6,69	0,12	0,87	2,24	0,16	0,10	0,07	1,24	69,78
A:7	0,16	0,47	11,22	8,16	0,59	0,87	3,51	0,11	0,14	0,11	0,69	73,52
A:8	0,29	0,12	16,57	3,53	0,07	0,35	1,92	0,15	0,08	0,08	0,60	76,04
A:9	0,79	0,28	18,08	5,95	0,41	0,64	3,14	0,11	0,14	0,14	0,72	69,42
B:1	0,36	0,68	15,73	7,32	0,74	0,36	2,79	0,16	0,11	0,14	0,58	70,75
B:2	0,41	0,42	8,16	8,16	0,26	0,38	2,92	0,14	0,12	0,09	0,56	78,12
B:3	0,39	0,38	27,12	8,08	0,56	0,39	2,70	0,19	0,12	0,05	0,75	59,04

[10] L. K. Herrera Quintero, *Physico-chemical research of cultural heritage materials using microanalytical methods*, Seville, 2009, p. 148.
[11] A.V. Ramesh Kumar, R. Balasubramaniam, *Corrosion product analysis of corrosion resistant ancient Indian iron*, în Corrosion Science, Vol. 40, Issue 7, 1998, p. 1171.
[12] Payman Roonasi, *Adsorption and Surface Reaction Properties of Synthesized Magnetite Nano-Particles*, Sweden, 2007, p. 36.

B:4	0,47	0,27	14,95	6,69	0,61	0,32	1,91	0,16	0,13	0,07	0,37	73,84
B:5	0,55	0,30	21,43	3,26	0,35	0,59	2,24	0,15	0,15	0,10	0,55	70,15
C:1	0,30	0,31	11,86	11,67	0,28	0,71	3,06	0,08	0,13	0,09	0,56	70,80
C:2	0,47	0,67	15,05	7,32	0,22	0,87	1,78	0,11	0,14	0,07	0,37	72,77
C:3	0,36	0,47	14,73	12,32	0,56	0,64	2,52	0,16	0,17	0,11	0,75	67,05
C:4	0,29	0,42	11,07	10,05	0,58	0,36	2,92	0,17	0,11	0,05	0,56	73,26

In all research, carbon varied between 0,02% (ferite) and 0,45%. So, all objects are in class hipoeutectoide steels (<0.8% C). Carbon concentration varies from one object to another but from one area to another of the same object.

Corroborating the results SEM with those obtained by metallographic analysis, could thus conclude that the inclusions are composed, in special, of phase type silicates (eg. Fe_2SiO_4) and iron sulphide and FeO (Wüstite type).

It also presented a classical aspect dense corrosion products, in gray matrix, traversed by clear marbly. These marbly can be or not connected to the metal and can present, the same sample, different shades of color, related to different phases or thickness or concentration heterogeneity.

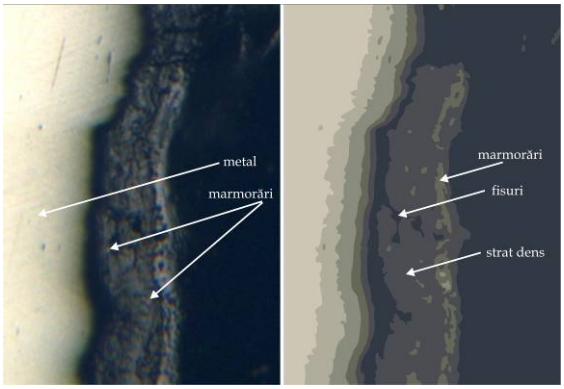

Fig. 36. Optical micrography presenting marbly inside layer of corrosion

The micrography obtained, combined wit SEM results, allowed us identification two factors that favor localized corrosion

1. due and along inclusions (eg. sample B:1)

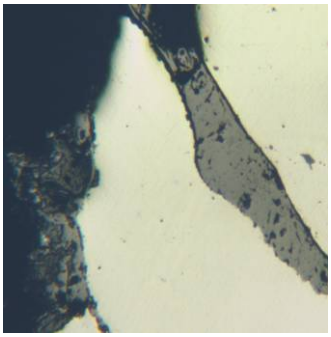

Fig. 37. Corrosion due and along inclusions

- Other causes (eg. sample A:3) This type of corrosion can be given to the presence of inclusions currently invisible or missing, which caused local corrosion advancement.

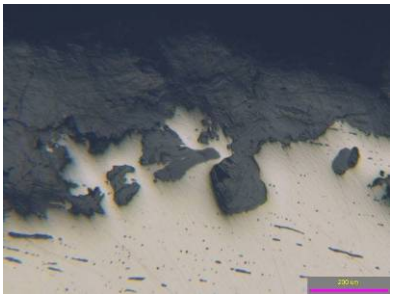

Fig. 38. Corrosion due to the presence of inclusions invisible or missing at time of analysis

FT-IR spectra of samples in the first group we have the following results:

Nr. probă / compus al ruginii	1	2	3	4	6	7	8	9
Goethite	880 784	624 794 882	784 875	883 794	796 881	790 882		780
Lepidocrocite	1027	1024		1019		1020		
Akaganeită						721		
Ferihidrită	460	459		460	456	458		
Maghemită							707	
Magnetită					613			
Hematită	533							
Carbonați	1418 1328	1414 1450	1322		1456	1465		1320 1462
Vibrații molec apă sau SH alungit	1632	1628	1641	1629	1631	1637	1696	1623
Apă	3417	3372	3400	3157	3417	3405	3348	3408
Sulfați								1111
Silicați şi filosilicați		670	461 608 672			672		461 1033
Hidrocarburi	2848 2923	2853 2923	2853 2924	1385 2853 2923	2853 2921	1384 2848 2919	830 1514 2870 2934	2849 2917
Fosfați			1039	1093				
Nitrați		1380	1395				1384	
Compuşi celulozici			1104		1104	1109	1036 1173 1240	
Fosfat feric			1166			1168		
Carbonat feric						1580		
$CaSO_4$, $2H_2O$								600 673

To identify certain products, To identify certain products to appeal to overlapping spectrum of samples 8 and 9, the standard spectra for two types of materials commonly used in restoration: Duroxan and paraffin wax. This led us to identify clearly the existence of one of the two materials. However it is difficult to determine exactly which one was used or both. The second variant, according to conservation-restoration would require the existence of two phases of conservation, which is less likely. So the view that has been used only one of them, most likely paraffin wax.

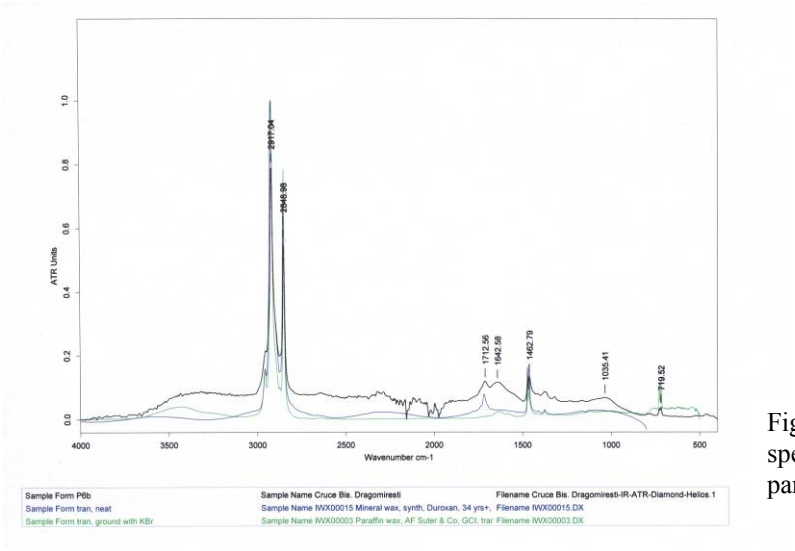

Fig. 39. Sample A:9 spectrum overlapped spectra Duroxan standard solution and the paraffin wax (analyzed in KBr pill)

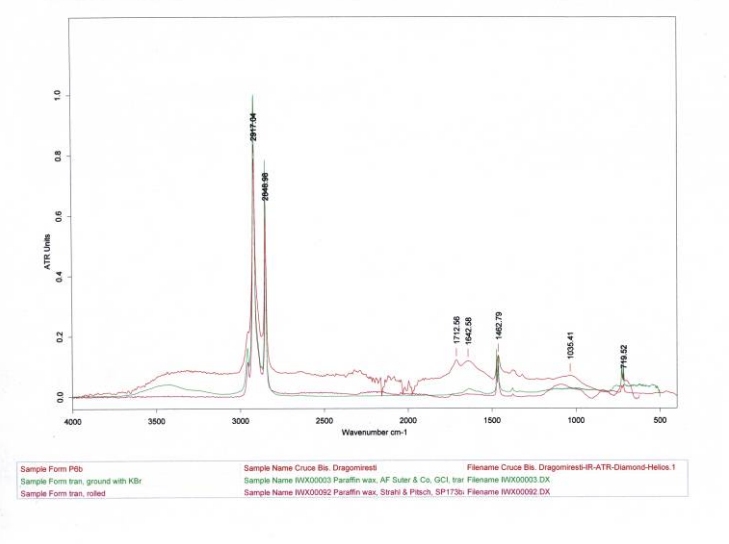

Fig. 40. Sample A:9 spectrum overlapped spectra standard the paraffin wax

Relationship created between iron and wood, in many cases, demonstrated the destructive effect of the first. But back there, the interaction between the two proves just as damaging to both. Corrosion of fasteners combined with wood damage, cause loss of common power and thus produces weakening the overall structural integrity.

FT-IR results for the second group are presented in the table below:

	1a	1b	2a	2b	3a	3b	4	5
Goethite	791 883	787 885	795 881	473 797 880	798 884	796 882	797 878	795 882
Lepidocrocite	1027	1028	1024		1024			1020
Ferihidrită	453	460			468	456		459
Magnetită					412 508			
Maghemită				603	605			596
Hematită			450					
Carbonați	1414	1315 1413	1414	1317 1405	1320 1417	1323 1418		1433
Vibrații molec apă sau SH alungit	1630	1631	1632	1641	1644	1637	1649	1643
Apă	3412	3403	3382	3382	3161	3196	3171	3124

Clorură ferică					667	666	665	
Sulfați					1115	1109	1112	1111
Hidrocarburi	2853 2923	2851 2928	2859 2932	2848 2923				
Nitrați				1365				
Fosfați	1093			1090				

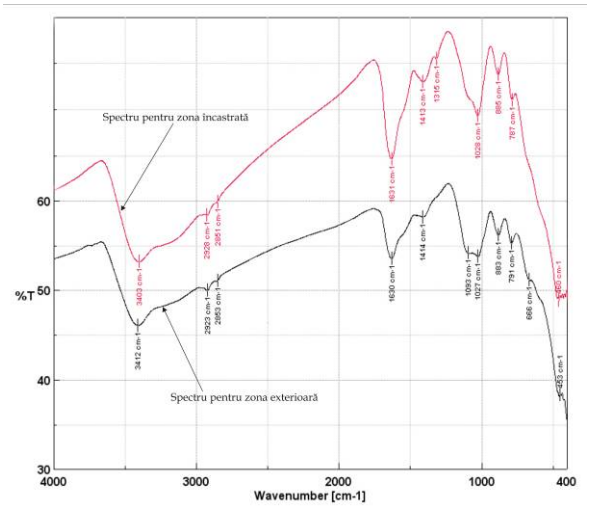

Fig. 41. Sample B:1 Representation of spectra for two areas: external - black line, embedded - red line.

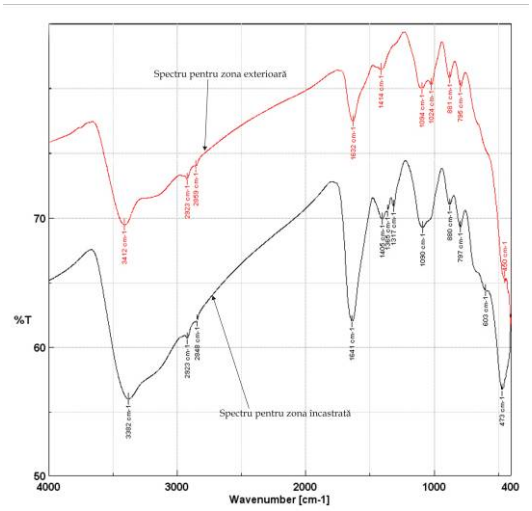

Fig. 42. Sample B:2 Representation of spectra for two areas: embedded - black line, exterior - red line.

Fig. 43.
Sample B:3, detail the middle area, where switching to the area was embedded in the outer

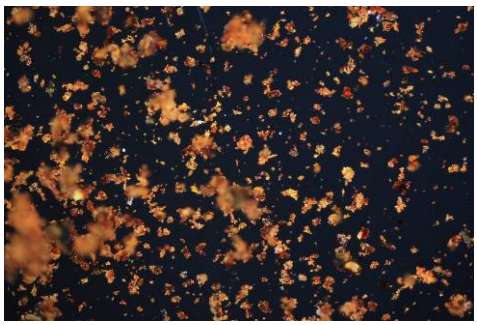

Fig. 44. Sample B:3a
in crossfire epipolarized light (100x). Is observed particles of yellow-ocher and red-orange, characteristic of a mixture of goethite and lepidocrocite

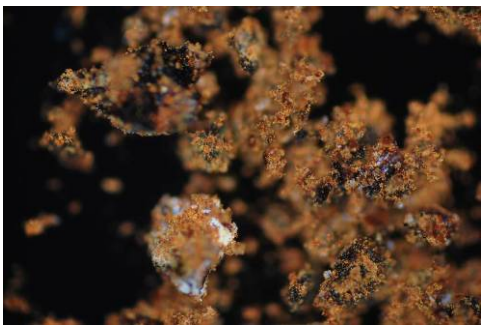

Fig. 45. Sample B:3b
in crossfire epipolarized light (100x). Observe crusty metal particles coated with yellow-ocher, brown, orange and white (typical goethite and carbonates)

For the III group, FT-IR spectra results were presented in the table below:

	C : 1	C : 2	C : 3	C : 4
Goethite	795 885	790 875	795 891	795 880
Lepidocrocite		1025		
Ferihidrită	464	459	453	464
Rugină verde	674	672		672
Carbonați	1317 1414	1328 1456	1418 1456	1072 1456
Vibrații molec apă sau SH alungit	1630	1641	1644	1462
Apă	3398	3389	3412	3432
Sulfați	1115			
Hidrocarburi	1376 2853 2923	2853 2923	619 1334 1384 2859 2923	2859 2923
Compuşi celulozici			1109	
Fosfat feric			662 1034	1030
Fosfați	1056		1264	
Inele aromatice			1509	
Ioni de amoniu (NH4+)		1406		1403
Carboxilați		1563		

Was observed for all three types of corrosion a massive presence of goethite and lepidocrocite. Interestingly peak at 1115 cm^{-1} appeared in the C : 1 sample spectrum. It can be attributed to sulfate absorbed magnetite particles.

Next, a comparison was made between the two types of embedded atmospheric corrosion:

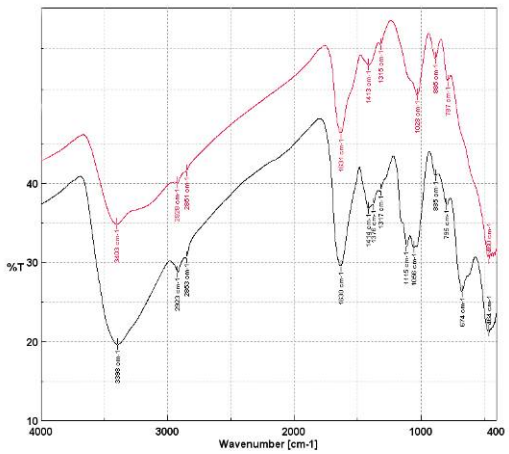

Fig. 46. Embedded areas spectra for : C: 1 - black line, B: 1b - red line

Comparing the spectra for the embedded atmospheric corrosion, and those from the indoor, embedded atmospheric corrosion, several similarities can be observed but also differences like:

- around the value of 670 cm^{-1} – attributed to the green rust, for the embedded area sample, exterior-atmospheric corroded, only a weak shoulder can be observed, while for the embedded, corroded in indoor atmosphere sample, a strong peak appears;

- hydro-carbonates, with values around 2850 cm^{-1}, 2920 cm^{-1}, are much more highlighted for the C:1 sample comparatively to the B:1b sample;

- for the lepidocrocite area (around the value of 1020 cm^{-1}), sample B:1b has a very well marked peak while the C:1 sample is most probably masked by the 1115 cm^{-1} peak, which can be attributed to the sulfate absorbed in the megnethite particles.

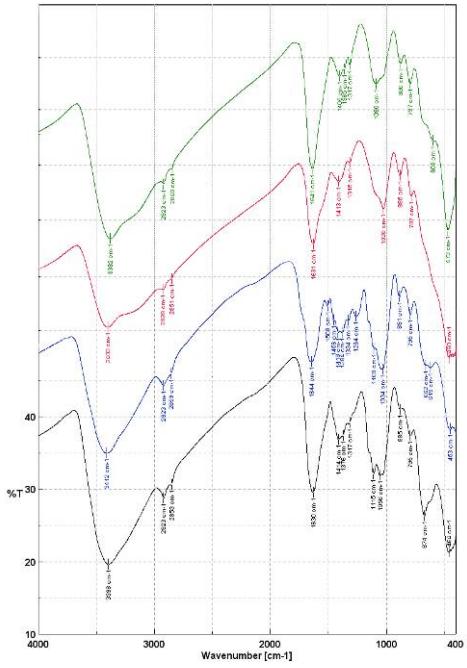

Fig. 47. Sample: line black – C:1; line blue – C:3; line red – B:1b; line green – B:2b

Using Figure 47, the differences for four spectra were highlighted, two for the recessed area being under the influence of indoor corrosion, and two for recessed area being under the influence of exterior atmospheric corrosion:

- spectral analysis showed that magnetite is present in the corrosion layer of the indoor atmospheric corrosion. The presence of magnetite involve a greater resistance to this type of corrosion as compared to outdoor atmospheric corrosion;
- It appears that the corrosion products, endogenous and exogenous, influences much more powerful recessed outdoor atmospheric corrosion, as compared to the recessed indoor atmospheric corrosion;
- the water quantity present in the corrosion products is close for the two situations, we estimate, due to the fact that the pieces from group C come from a constant wet and chilly atmosphere.

Personal contributions:

- studying, for the first time in Romania, the long-term atmospheric corrosion (100-200 years), having as samples ethnographic objects;
- approaching the subject depending on three situations in which atmospheric corrosion occurs: free-exterior, embedded-exterior, embedded-indoor;
- identifying the major compounds present in the corrosion layer, produced in the three situations;
- comparing the corrosion products resulted from the two embedding situations analyzed.